2014

On the 3-D structure and dissipation of reconnection-driven flow bursts

J. F. Drake

M. Swisdak

P. A. Cassak

T. D. Phan

On the 3-D structure and dissipation of reconnection-driven flow-bursts

J. F. Drake and M. Swisdak

University of Maryland, College Park, MD 20742, USA

P. A. Cassak

West Virginia University, Morgantown, WV 26506, USA

T. D. Phan

University of California, Berkeley, CA 94720, USA

(Dated: June 27, 2018)

Abstract

The structure of magnetic reconnection-driven outflows and their dissipation are explored with large-scale, 3-D particle-in-cell (PIC) simulations. Outflow jets resulting from 3-D reconnection with a finite length x-line form fronts as they propagate into the downstream medium. A large pressure increase ahead of this "reconnection jet front" (RJF), due to reflected and transmitted ions, slows the front so that its velocity is well below the velocity of the ambient ions in the core of the jet. As a result, the RJF slows and diverts the high-speed flow into the direction perpendicular to the reconnection plane. The consequence is that the RJF acts as a thermalization site for the ion bulk flow and contributes significantly to the dissipation of magnetic energy during reconnection even though the outflow jet is subsonic. This behavior has no counterpart in 2-D reconnection. A simple analytic model predicts the front velocity and the fraction of the ion bulk flow energy that is dissipated.

Magnetic reconnection is the dominant mechanism for dissipating magnetic energy in large-scale plasma systems and is the driver of explosive events such as flares in astrophysical systems and flow bursts in the Earth's magnetosphere. Most of the energy released during reconnection takes place not at the x-line but downstream in the exhaust where newly reconnected field lines relax their magnetic tension. In the MHD description the Petschek shocks that bound the exhaust both drive the Alfvénic exhaust and heat the upstream plasma entering the exhaust [1, 2]. In the nearly collisionless environment of many systems, while the exhaust outflow is close to the MHD prediction [3], the exhaust heating results from counterstreaming ions [4, 5] rather than Petschek shocks. The kinetic energy of the bulk flow driven during reconnection is a substantial fraction of the released magnetic energy and in natural systems this energy is ultimately dissipated. However, the dominant processes that control the dissipation of these flows and their universality have not yet been established.

During solar flares the termination shock that has been observed at the low altitude edge of coronal reconnection exhausts [6] is a possible mechanism for the dissipation of the energy in the bulk flow. Supra Arcade Downflows (SADs) [7], which are believed to be driven by reconnection, are observed to slow during their downward trajectory toward the solar surface. In the Earth's magnetotail a key observational discovery was the formation of narrow boundary layers or fronts at the interface of the high-speed reconnection jets and the essentially stationary ambient plasma downstream. At the front the amplitude of the magnetic field normal to the initial current layer (B_z in the magnetotail) increases abruptly [8–10]. Initially such fronts (dubbed "dipolarization fronts") were believed to result from the slowing of the reconnection outflow as it impacted the strong dipole field of the Earth, similar to coronal termination shocks. However, the measured propagation of these fronts over large distances both Earthward and tailward of the reconnection site [8, 11] is strong evidence that these fronts are generically associated with the development of reconnection in natural systems and are not specific to the geometry of a particular system.

The role that reconnection jet fronts (RJFs) play is, however, unclear. It has been suggested that RJFs may be important sites for energy dissipation [11–13]. A number of 2-D reconnection simulations (corresponding to an infinite length x-line) have been carried out to explore the structure of RJFs [14, 15]. On the other hand, it is unlikely that reconnection in physical systems is 2-D since reconnection very likely onsets in a spatially localized region. Flow-bursts and associated RJFs in the magnetotail are localized in the cross-tail (y) direc-

tion with characteristic scales of several Earth radii R_E [16, 17] and therefore correspond to finite length x-lines. SADs have similarly been interpreted as resulting from reconnection with finite length x-lines [18, 19]. We show that the structure of the exhaust and its dissipation depends critically on its 3-D structure.

Since we are focusing on the structure of the reconnection outflows and the associated RJF and not on the structure of the dissipation region where field lines change topology, we explore the dynamics with the Riemann approach [2]. Consistent with the observations, we study how reconnection develops in a 3-D model with a finite x-line by imposing a spatially localized region of reconnected flux B_z on top of a Harris current sheet. A PIC model is used so that the collisionless dissipation of reconnection-driven flows can be studied. The system is initially in pressure balance but the curvature forces that drive reconnection are unbalanced and drive the outflow. A large pressure increase ahead of the front, due to reflected and transmitted ions, slows the front so that its velocity is well below the velocity of the ambient reconnection outflow. As a result, the front slows and diverts the outflow into the ion drift direction of the downstream current layer. The front, therefore acts as a thermalization site for the energy of the flow. A simple model illustrates how the energy in the flow is dissipated and is proposed as a prototype for understanding how reconnection-driven flows are dissipated in nature. No significant enhancement in electron dissipation takes place at the front.

We explore a system periodic in three directions: with $x - z$ the plane of reconnection and the reconnection outflow along x. Superimposed on a double Harris current layer $B_x(z)$ with a half-width of $2.0d_i$ (with d_i the ion inertial length) is a region of uniform magnetic flux $B_z(x, y)$ that is localized in the $x - y$ plane as shown in Fig. 1(a). The density in the region of $B_z \neq 0$ is reduced to the background density n_0 of the Harris system. The electron and ion temperatures are adjusted so that the total pressure is balanced with $T_i/T_e = 5$, which is typical for the magnetosphere. Required currents are carried by both species, in proportionality to their temperature. Unbalanced forces associated with magnetic tension will drive the plasma in the region of $B_z \neq 0$ to the left in Fig. 1(a). The results of our PIC simulations are presented in normalized units: the magnetic field to the asymptotic value B_0 of the Harris reversed field, the density to the value at the center of the current sheet minus $n_0 = 0.3$, velocities to the Alfvén speed c_A, lengths to d_i, times to the inverse ion cyclotron frequency Ω_{ci}^{-1}, and temperatures to $m_i c_A^2$. The computational domain is

$102.4d_i \times 25.6d_i \times 25.6d_i$. Other parameters of the simulations are a mass-ratio $m_i/m_e = 25$, which is sufficient to separate the dynamics of the two species [20], and speed of light $c = 15c_A$.

Shown in Fig. 1 is B_z in the center of the current sheet ($z = 0$) at (a) $t = 0$, (b) $t = 12\Omega_{ci}^{-1}$ and (c) $t = 24\Omega_{ci}^{-1}$. The outflow carries the flux B_z to the left propelled by the unbalanced magnetic curvature forces that drive reconnection. The corresponding flow v_{ix} at $t = 24\Omega_{ci}^{-1}$ is shown in Fig. 2(a). A surprise in this data is the strong positive flow just below the main flow in a region where $B_z \sim 0$ and there is therefore no curvature. The reason for this flow is discussed later. In the core of the flow jet the flux B_z is carried upward in Fig. 1, which is in the electron drift direction (Fig. 2(b)), and is compressed at the upper edge. In contrast, the left edge of the jet turns towards downward, which is in the ion drift direction (Fig. 2(c)). Similar turning in the ion drift direction was seen in 3-D PIC simulations of interchange turbulence in the magnetotail [21]. The motion downward at the front of the jet is due to an electric field E_x directed to the right which causes both species to drift downward (Figs. 2(b)-(d)). The asymmetry of the structure of the jet in the y-direction is contrasted with the results of an MHD simulation with nearly identical initial conditions (the minimum density is slightly higher in the MHD case) in which the jet forms a symmetrical structure in the $x - y$ plane (Fig. 1(d)). These MHD flows are similar to those from earlier 3-D MHD simulations of plasma interchange-driven flows in the magnetotail [22].

In Fig. 3 are cuts of the ion density (solid), B_z (dotted) and the ion velocity v_{ix} (dashed) versus x in the center of the current sheet at $t = 24\Omega_{ci}^{-1}$. The density drops sharply across the front and into the jet although the density minimum of around 0.7 is well above the initial condition of 0.3. B_z rises sharply across the front and exhibits the distinctive dip and overshoot that are often seen in the observations [8, 9]. The overshoot results from local compression at the front, which produces a similar peak in the density. The region of negative B_z ahead of the front can also be seen as the white region in Fig. 1(c) in the interval $-35d_i < x < -25d_i$ and $-9d_i > y > -13d_i$. The mechanism for this reversal in B_z appears to be similar to the self-generation of magnetic fields in the Weibel instability and will be discussed more fully in a separate publication.

The ion velocity rises gradually ahead of the front as in observations and reaches a plateau around $0.8c_A$, which is well below that expected based on the upstream Alfvén speed ($1.8c_A$). The velocity v_f of the front is around $0.46c_A$ and is calculated by stacking cuts of B_z versus

x at several times (Fig. 4). The reduced velocity of the front compared with that of the core of the jet results from the buildup of ion pressure ahead of the front shown in Fig. 2(e). The increase in pressure is largest at the top corner of the front and serves to both slow the jet and deflect it downward. Such pressure enhancements have been documented in satellite measurements [23]. The pressure increase is a consequence of the reflection of ions in the current sheet off of the head of the front, which has also been documented in satellite observations [24] and discussed in 2-D reconnection models [15]. The penetration of high velocity ions in the jet through the front also contributes to the pressure increase. Both classes of particles can be seen to the left of the front in the $x - v_x$ phase space in Fig. 5(a), which is from the center of the current sheet with $y = -11.8d_i$ and $t = 20\Omega_{ci}^{-1}$. The cut of B_z in Fig. 5(b) shows the location of the front. As expected, the reflected ions have a velocity close to c_A, which is around twice v_f. In Fig. 2(f) is the ion temperature T_{ixx} corresponding to the pressure in Fig. 2(e). The increase in ion temperature associated with the reflected ions is evident.

The mechanism that produces the enhanced ion temperature below the jet and to the right of the front is also responsible for the strong leftward-directed flow in the same region shown earlier in Fig. 2(a). Ions moving to the left in the core of the jet also drift downward (Fig. 2(c)) and eventually exit the region of strong B_z into the adjacent stationary plasma. These ions continue to flow to the left through the stationary background ions. The resulting counterstreaming ion velocity distributions in this region where $B_z \sim 0$ have a net drift to the left (Fig. 2(a)) and produce an effective T_{ixx} as seen in Fig. 2(f). A cut along x at $y = -10d_i$ (not shown) reveals a localized peak in B_z at the front but with a flow to the left that remains large well to the right of the front where $B_z \sim 0$. Such behavior has been documented in THEMIS magnetotail observations [13]. In contrast with the ions, we have measured no significant increase in the electron temperature at the front (Fig. 2(g)) in spite of the intense electron current in the $x - y$ plane that produces the rather complex magnetic structure B_z in Fig. 1.

Before further addressing the properties of the front, we emphasize that this sharp boundary is not a shock. First, in the upstream region to the right of the front the fast-mode phase speed based on the total plasma and magnetic pressure is around $1.0c_A$ while the flow speed of the jet is around $0.8c_A$ so the upstream Mach number is less than unity. Further, if the front were a shock, the flow through the shock would carry the flux B_z across the shock into

the downstream region, which is not seen in the simulation data. Nevertheless, while the front is not a shock, that the velocity in the core of the flow-burst is substantially higher than that of the front has important implications for understanding the dissipation of reconnection driven flows. The plasma within the jet eventually catches up to the front where it is compressed and deflected with reduced velocity downward in Fig. 2(c). The consequence is that the integrated volume of plasma behind the flow-burst (measured by the reduction in the size of the non-zero B_z region) decreases with time. This can be seen in Figs. 1(b)-(c). The integrated magnetic flux B_z in the jet is decreasing with time and the corresponding flux convecting downward is increasing (Fig. 1). Thus, the front is more than simply the front edge of the jet. Rather, it is the site for conversion of flow energy into ion thermal energy and much of the plasma that makes up the jet will be directly processed within the front.

A simple analytic calculation illustrates how the reduction in flow energy takes place. We consider a simple 2-D system in the $x-y$ plane in which the plasma in the current sheet (density n_{cs}) interacts with the plasma in the jet (density n_b). The front and jet velocities are v_f and v_b, respectively, while the current sheet ions are at rest. For simplicity, we ignore the ambient drift along y, which adds complexity to the calculation but does not change the final result. In the frame of the front, ions in the current sheet move with a velocity $-v_f$ along x, are reflected by the magnetic boundary and leave the front with a velocity v_f. The jet ions have an incident velocity $v_b - v_f$ and are deflected into the y direction with their speed unchanged. Force balance at the front, neglecting the residual magnetic stress, yields $2n_{cs}v_f^2 = n_b(v_b - v_f)^2$, which can be solved for the front velocity $v_f = Rv_b/(1+R)$ where $R = \sqrt{n_b/2n_{cs}}$. In the frame of the front, neither the current sheet nor the jet ions change energy. In the simulation frame, however, there is a transfer of energy from the jet ions to the current sheet ions. The change in energy $\Delta W = W_f - W_i$ of the jet ions is given by

$$\Delta W = \frac{1}{2} m_i n_b (v_f^2 + (v_b - v_f)^2 - v_b^2) = -2W_i \frac{R}{(1+R)^2}. \quad (1)$$

with $W_i = m_i n_b v_b^2/2$. This energy loss corresponds to the energy gain of the current sheet ions. Thus, the fraction of energy conversion is linked to the density ratio between the jet and current sheet ions. In the limit of $n_b/n_{cs} \to 0$ there is no energy conversion. For a typical value $n_b/n_{cs} = 0.2$ [9] the fraction of energy conversion is 0.37 according to this simple model. The model, of course, greatly simplifies a very complex system. The model

prediction of the front velocity in the simulation is $0.3c_A$ compared with the measured value of $0.46c_A$. Finally, we emphasize that the deflection of the jet into the y direction has no counterpart in a 2-D reconnection model.

Estimates of the front velocity based on multi-spacecraft THEMIS observations have been presented [10] but a direct comparison with the velocity of the core of the jet has not been carried out. This comparison would be facilitated if a local measure of the velocity of the front from single spacecraft data could be obtained. From the simulation we have evaluated the local $\mathbf{E} \times \mathbf{B}$ velocity at the peak of B_z. At $t = 30\Omega_{ci}^{-1}$ this velocity is $0.47c_A$, which is quite close to the value of $0.46c_A$ deduced from the stack of plots in Fig. 4. The local ion velocity v_{ix} at the peak of B_z is also close to but somewhat higher than the front velocity.

The overshoot in B_z seen in many observations of RJF encounters in the magnetotail is already evidence of the pileup of the jet plasma at the front but direct comparisons of the front velocity with that of the core of the jet are necessary to test the ideas presented here. While the focus of the present paper is on reconnection-driven jets, jets driven by the magnetized Rayleigh-Taylor instability [25] or other mechanisms might also exhibit similar deflections and associated dissipation of bulk flow energy.

The authors would like to thank V. Angelopoulos and A. Runov and L. S. Shepherd for helpful discussions. This work was supported in part by NASA grants NNX14AC78G, NNX08AO83G and NNX10AN08A and NSF Grants ATM-0903964 and AGS-093463. Computations were performed at the National Energy Research Scientific Computing Center and on NASA Advanced Supercomputing Division resources.

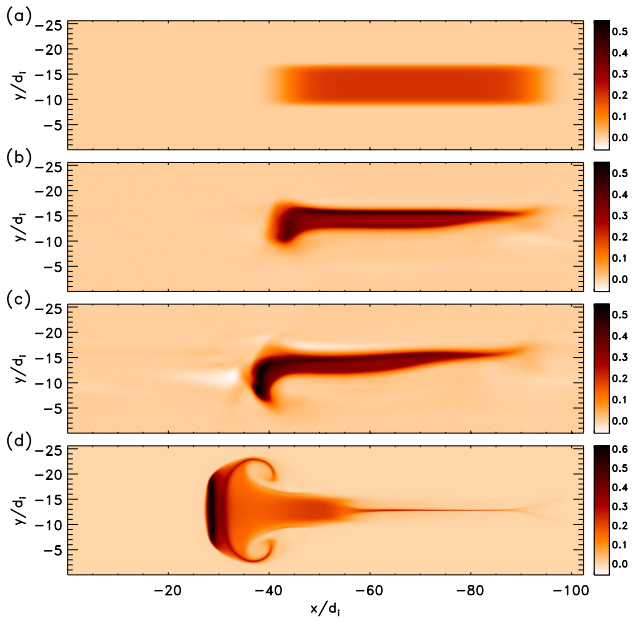

FIG. 1. (Color online) From the PIC simulation plots of B_z in the $x-y$ plane at the center of the current sheet ($z=0$) at (a) $t=0$, (b) $t=12\Omega_{ci}^{-1}$ and (c) $t=24\Omega_{ci}^{-1}$. In (d) a similar plot from an MHD simulation with nearly identical initial conditions at the same time as in (c).

[1] H. E. Petschek, in *AAS/NASA Symposium on the Physics of Solar Flares*, edited by W. N. Ness (NASA, Washington, DC, 1964), p. 425.

[2] Y. Lin and L. C. Lee, J. Geophys. Res. **100**, 19227 (1995).

[3] B. U. Ö. Sonnerup, G. Paschmann, I. Papamastorakis, N. Sckopke, G. Haerendel, S. J. Bame, J. R. Asbridge, J. T. Gosling, and C. T. Russell, J. Geophys. Res. **86**, 10049 (1981).

[4] M. Hoshino, T. Mukai, and T. Yamamoto, J. Geophys. Res. **103**, 4509 (1998).

[5] J. T. Gosling, R. M. Skoug, and D. J. McComas, Geophys. Res. Lett. **110**, A01107 (2005).

[6] S. Masuda, T. Kosugi, H. Hara, S. Tsuneta, and Y. Ogawara, Nature **373**, 495 (1994).

[7] D. E. McKenzie and H. S. Hudson, Astrophys. J. Lett. **519**, 93 (1999).

[8] S.-I. Ohtani, M. A. Shay, and T. Mukai, J. Geophys. Res. **109**, A03210 (2004).

[9] A. Runov, V. Angelopoulos, M. I. Sitnov, V. A. Sergeev, J. Bonnell, J. P. McFadden, D. Larson, K.-H. Glassmeier, and U. Auster, Geophys. Res. Lett. **36**, L14106 (2009).

[10] A. Runov, V. Angelopoulos, X.-Z. Zhou, X.-J. Zhang, S. Li, F. Plaschke, and J. Bonnell,

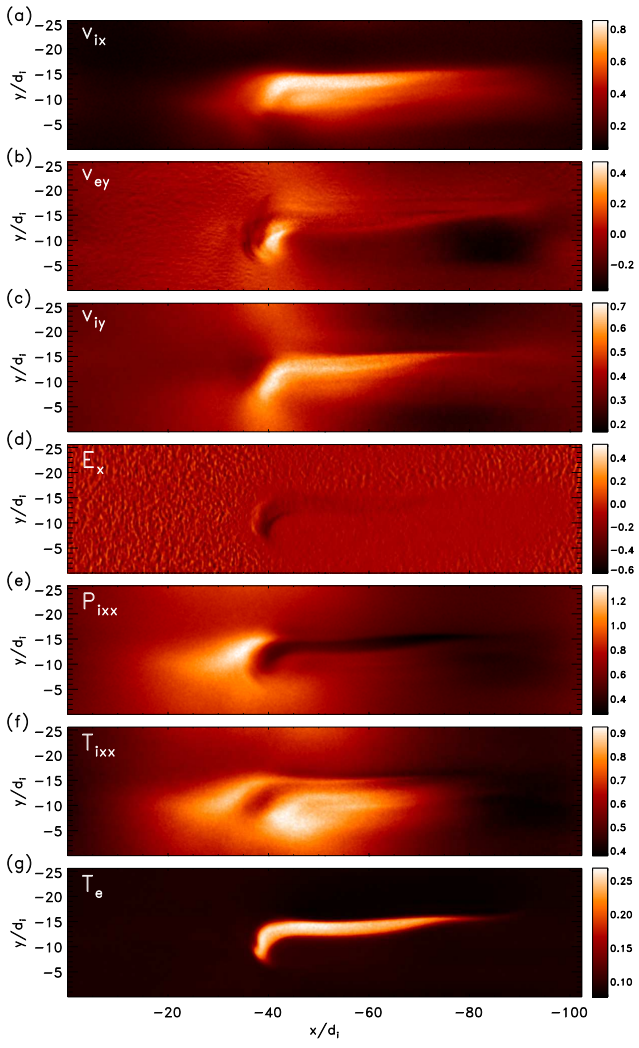

FIG. 2. (Color online) As in Fig. 1 at $t = 24\Omega_{ci}^{-1}$ plots of (a) v_{ix}, (b) v_{ey}, (c) v_{iy}, (d) E_x, (e) p_{ixx}, (f) T_{ixx} and (g) T_e.

Journal of Geophysical Research (Space Physics) **116**, A05216 (2011).

[11] V. Angelopoulos, A. Runov, X.-Z. Zhou, D. L. Turner, S. A. Kiehas, S.-S. Li, and I. Shinohara, Science **341**, 1478 (2013).

[12] M. Hoshino, T. Mukai, T. Terasawa, and I. Shinohara, J. Geophys. Res. **106**, 25979 (2001).

[13] A. Runov, V. Angelopoulos, M. Sitnov, V. A. Sergeev, R. Nakamura, Y. Nishimura, H. U. Frey, J. P. McFadden, D. Larson, J. Bonnell, et al., Planetary & Space Sci. **59**, 517 (2011).

[14] M. I. Sitnov, M. Swisdak, and A. V. Divin, J. Geophys. Res. **114**, A04202 (2009).

[15] P. Wu and M. A. Shay, Geophys. Res. Lett. **39**, L08107 (2012).

[16] V. Angelopoulos, T. D. Phan, D. E. Larson, F. S. Mozer, R. P. Lin, K. Tsuruda, H. Hayakawa,

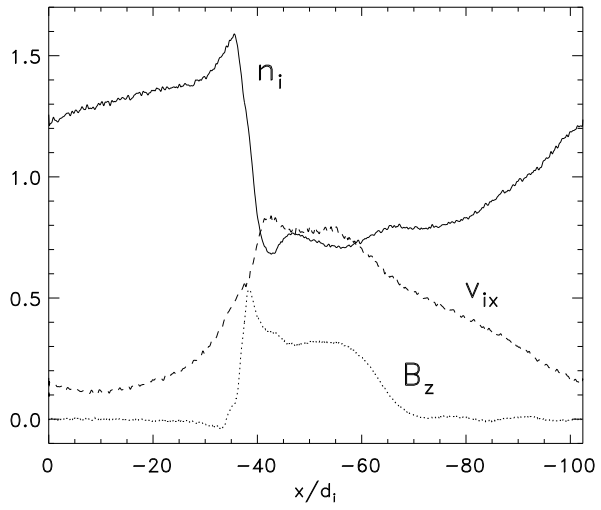

FIG. 3. Cuts of the ion density n_i (solid), v_{ix} (dashed) and B_z (dotted) along x at $z = 0$ and $y = -11.3d_i$ at the same time as in Fig. 2.

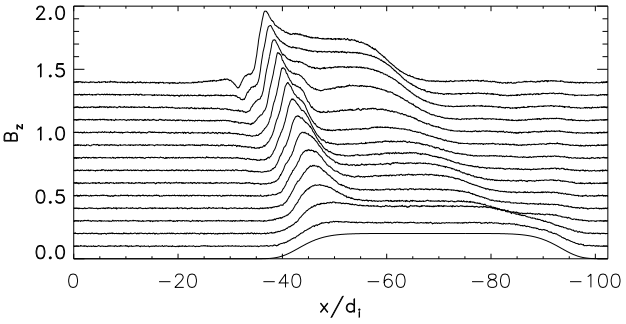

FIG. 4. A stack of cuts of B_z along x at $z = 0$ and $y = -11.3d_i$ separated by time intervals of $2\Omega_{ci}^{-1}$ starting from $t = 0$. The velocity of the front calculated from the peaks of B_z is $0.46c_A$.

T. Mukai, S. Kokubun, T. Yamamoto, et al., Geophys. Res. Lett. **24**, 2271 (1997).

[17] R. Nakamura, W. Baumjohann, C. Mouikis, L. Kistler, A. Runov, M. Volwerk, Y. Asano, Z. Vörös, T. L. Zhang, B. Klecker, et al., Geophys. Res. Lett. **31**, 9804 (2004).

[18] M. G. Linton and D. W. Longcope, ApJ **642**, 1177 (2006), astro-ph/0509348.

[19] P. A. Cassak, J. F. Drake, J. T. Gosling, T. Phan, M. A. Shay, and L. S. Shepherd, ApJ Lett. **775**, L14 (2013).

[20] M. Hesse, K. Schindler, J. Birn, and M. Kuznetsova, Phys. Plasmas **5**, 1781 (1999).

[21] P. L. Pritchett and F. V. Coroniti, J. Geophys. Res. **118**, 146 (2013).

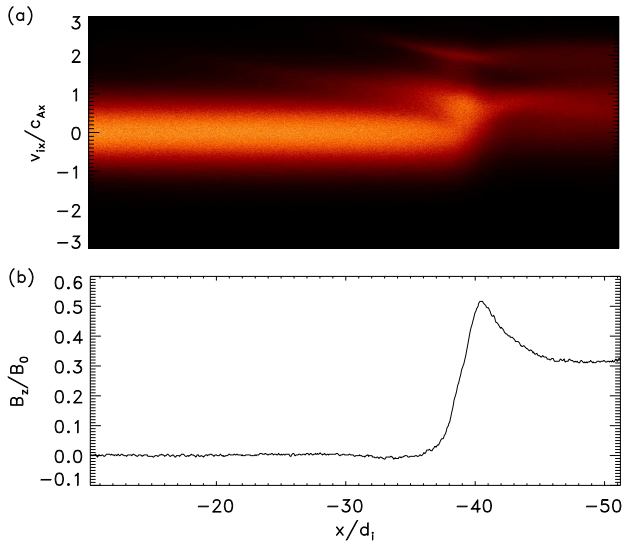

FIG. 5. (Color online) In (a) the ion phase space $v_x - x$ in the center of the current sheet at $y = -11.3d_i$ and $t = 20\Omega_{ci}^{-1}$. In (b) a cut of B_z at the same time and location.

[22] J. Birn, J. Raeder, Y. Wang, R. Wolf, and M. Hesse, Annales Geophysicae **22**, 1773 (2004).

[23] J. Liu, V. Angelopoulos, X.-Z. Zhou, A. Runov, and Z. Yao, Journal of Geophysical Research (Space Physics) **118**, 7104 (2013).

[24] X.-Z. Zhou, V. Angelopoulos, V. A. Sergeev, and A. Runov, Journal of Geophysical Research (Space Physics) **115**, A00I03 (2010).

[25] J. Birn, M. F. Thomsen, and M. Hesse, Annales Geophysicae **22**, 1305 (2004).